agronomy

MDPI

Article

OsVTC1-1 RNAi Mutant with Reduction of Ascorbic Acid Synthesis Alters Cell Wall Sugar Composition and Cell Wall-Associated Proteins

Kanyanat Lamanchai [1], Deborah L. Salmon [2], Nicholas Smirnoff [2], Pornsawan Sutthinon [3], Sittiruk Roytrakul [4], Kantinan Leetanasaksakul [4], Suthathip Kittisenachai [4] and Chatchawan Jantasuriyarat [1,5,*]

1 Department of Genetics, Faculty of Science, Kasetsart University, Chatuchak, Bangkok 10900, Thailand; kanyanat.lo@ku.th
2 Biosciences, College of Life and Environmental Sciences, University of Exeter, Exeter EX4 4QD, UK; d.l.salmon@exeter.ac.uk (D.L.S.); n.smirnoff@exeter.ac.uk (N.S.)
3 Department of Botany, Faculty of Science, Kasetsart University, Chatuchak, Bangkok 10900, Thailand; pornsawan.sut@ku.th
4 Functional Proteomics Technology, National Center for Genetic Engineering and Biotechnology, National Science and Technology Development Agency, 113 Paholyothin Road, Klong 1, Klong Luang, Pathumthani 12120, Thailand; sittiruk@biotec.or.th (S.R.); kantinan.lee@biotec.or.th (K.L.); suthathip@biotec.or.th (S.K.)
5 Center for Advanced Studies in Tropical Natural Resources, National Research University-Kasetsart University (CASTNAR, NRU-KU), Kasetsart University, Chatuchak, Bangkok 10900, Thailand
* Correspondence: fscicwj@ku.ac.th

Abstract: Ascorbic acid (AsA) or Vitamin C is an antioxidant molecule and plays an important role in many biological processes in plants. GDP-D-mannose pyrophosphorylase (GMP or VTC1) catalyzes the synthesis of GDP-D-mannose, which is a precursor for AsA production and is used for cell wall polysaccharide and glycoprotein synthesis. In rice, the *OsVTC1* gene consists of three homologs, including *OsVTC1-1*, *OsVTC1-3* and *OsVTC1-8*. In this study, we characterized wild type (WT) and *OsVTC1-1* RNAi lines (RI1-2 and RI1-3) and showed that the transcript levels of most genes in the AsA synthesis pathway, AsA content and leaf anatomical parameters in RNAi lines were reduced, revealing that *OsVTC1-1* is involved in AsA synthesis. To further study the role of *OsVTC1*-1 gene, cell wall monosaccharide composition, transcriptome and proteome were compared, with specific attention paid to their wild type and *OsVTC1-1* RNAi lines. Mannose and galactose composition (mole%) were decreased in *OsVTC1-1* RNAi lines. Additionally, reduction of cell wall-associated proteins, such as kinesin, expansin, beta-galactosidase and cellulose synthase were observed in *OsVTC1-1* RNAi lines. Our results suggest that *OsVTC1-1* gene plays an important role in AsA synthesis and in cell wall-related processes.

Keywords: antioxidant; GDP-D-mannose pyrophosphorylase; cell wall; ascorbic acid

Citation: Lamanchai, K.; Salmon, D.L.; Smirnoff, N.; Sutthinon, P.; Roytrakul, S.; Leetanasaksakul, K.; Kittisenachai, S.; Jantasuriyarat, C. *OsVTC1-1* RNAi Mutant with Reduction of Ascorbic Acid Synthesis Alters Cell Wall Sugar Composition and Cell Wall-Associated Proteins. *Agronomy* **2022**, *12*, 1272. https://doi.org/10.3390/agronomy12061272

Academic Editor: José-Luis Acebes

Received: 14 April 2022
Accepted: 24 May 2022
Published: 26 May 2022

1. Introduction

Ascorbic acid (AsA), or vitamin C, is a strong antioxidant molecule. AsA is required for multiple biological functions, for instance, the cofactors for enzyme activity, cell division, cross-linking of cell wall protein, photosynthesis, biotic and abiotic stresses and defense response [1–4]. Plants synthesize AsA mainly in photosynthetic tissues through the Smirnoff-Wheeler pathway via L-galactose [5,6]. There are several enzymes in the Smirnoff-Wheeler pathway, starting with phosphoglucose isomerase (PGI), which converts D-glucose-6-phosphate to D-fructose-6-phosphate, followed by phosphomannose isomerase (PMI), which converts D-fructose-6-phosphate to D-mannose-6-phosphate. Phosphomannose mutase (PMM), GDP-mannose pyrophosphorylase (GMP or VTC1), GDP-mannose-3′,5′-epimerase (GME), GDP-L-galactose phosphorylase (GGP or VTC2),

L-galactose-1-phosphate phosphatase (GPP or VTC4), L-galactose dehydrogenase (GDH) and L-galactono-1,4-lactone dehydrogenase (GLDH) are sequentially catalyzed into the final product, L-ascorbic acid [5]. Rice genomes contain one copy of *OsVTC2*, *OsVTC4* and *OsGDH* genes, but two copies of *OsGME* and *OsGLDH* and three copies of the *OsVTC1* gene [6]. GDP-D-mannose pyrophosphorylase (GMP or VTC1) is required for the conversion of D-mannose-1-phosphate to GDP-D-mannose [7]. Among three homologs of rice *OsVTC1*, *OsVTC1-1* is associated with the greatest AsA production in rice leaves, whereas *OsVTC1-3* plays a role in AsA synthesis in roots. *OsVTC1-8* may not be involved in AsA synthesis in both leaves and roots [8]. *vtc1* mutants have been broadly used to study functional roles in plants. In Arabidopsis, *vtc1* mutant has a smaller cell size than in the wild type [9]. Similarly, *vtc1* mutant exhibited reduced shoot growth and delayed flowering, supporting the idea that AsA is required for normal plant growth and development [10]. The *VTC1* gene is also involved in abiotic stress response. *OsVTC1-1* RNAi rice, which decreases the expression of the *OsVTC1-1* gene, exhibits reduced salt tolerance at both seedling and reproductive stages [11]. These reports indicate that the *VTC1* gene plays multiple roles in plants.

Two intermediates of the Smirnoff-Wheeler pathway, GDP-D-mannose and GDP-L-galactose, are also precursors of the non-cellulosic components of the plant cell wall. GDP-mannose-3′,5′-epimerase (GME) catalyzes the synthesis of GDP-L-galactose, a precursor for both AsA and cell wall polysaccharides synthesis [3]. GME was revealed to be involved in plant growth, leaf senescence and tolerance to acid, drought and salt in Arabidopsis [12,13]. VTC2 catalyzes the conversion of GDP-L-galactose to L-galactose-1-phosphate. This step is the first rate-determining step in AsA synthesis [14]. Next, VTC4, GDH and GLDH catalyze the formation of AsA via sugar intermediates, including L-galactose and L-galactono-1,4-lactone [5]. The role of these enzymes has been reported in many studies. For example, VTC2 plays a role in salt tolerance in rice [15]. The bacterium *Pseudomonas syringae* infection is restricted in *vtc2* mutant of Arabidopsis, indicating that VTC2 involves in defense response [9]. VTC4 is a bifunctional enzyme that affects the synthesis of both AsA and myo-inositol [16]. Moreover, glutathione peroxidases (GPX) is an antioxidation enzyme that reduces hydrogen peroxide (H_2O_2) to water against oxidative damage [17]. In this reaction, H_2O_2 is detoxified by GPX using hydrogens from reduced glutathione (GSH) resulting in water and oxidized glutathione (GSSG) that associates with the ascorbate-glutathione (ASA-GSH) cycle [18]. Due to antioxidant activity, GPX plays an essential role in various abiotic stress responses and defense mechanisms in plants [19].

Plant cell walls are important in their development and for environmental responses [20]. Cell wall polysaccharides, mainly contain of cellulose, hemicellulose and pectin, are built up of sugars by glycosidic linkages to form polymers [21]. Cellulose, a main component of the plant cell wall, is composed of β-(1,4)-D-Glucose residues [22]. Cellulose is synthesized by cellulose synthase complex that composed of different cellulose synthase (CESA) proteins [23]. Hemicellulose is composed of several different types of sugars. For example, Glucuronoxylan contains xylose and glucuronic acid (GlcA), and Galactomannan consists of mannose and galactose. The xylose backbone with arabinose is polymerized to arabinoxylan [24,25]. Pectin is mostly consisted of galacturonic acid (GalA) residues. It can be divided into different types, including homogalacturonan, xylogalacturonan, apiogalacturonan, rhamnogalacturonan I and rhamnogalacturonan II (RGII) [26]. The side chain of RGII consists of arabinose, apiose, fucose, galactose, rhamnose, aceric acid, glucuronic acid and xylose [27]. The plant cell wall is comprised of several different monosaccharides. In summary, mannose and galactose are required for both AsA synthesis as well as cell wall formation [7]. In this study, we examined the expression level of genes in the AsA synthesis pathway, AsA content, leaf anatomical structure and the monosaccharide composition of cell walls between wild type (WT) and *OsVTC1-1* RNAi lines. Transcriptome and proteome techniques were also used to analyze and compare genes and proteins between WT and *OsVTC1-1* RNAi lines. We confirmed that AsA synthesis genes and AsA content in *OsVTC1-1* RNAi lines are lower than in wild type. Moreover, mannose and galactose composition

as a percent mole of total sugars were significantly decreased in *OsVTC1-1* RNAi lines. Genes and proteins were differentially expressed, especially proteins involved in cell wall biosynthesis. Our results suggest that the *OsVTC1-1* gene is important in both AsA and cell wall biosynthesis. The obtained information will lead to a better understanding of the role of vitamin C in plants.

2. Materials and Methods

2.1. Plant Materials

Transgenic RNAi rice lines with reduced expression levels of an *OsVTC1-1* gene, including RI1-2 and RI1-3 lines, were obtained from Biotechnology Research Institute, Chinese Academy of Agricultural Sciences, Beijing, China. The japonica rice variety Zhonghua17 (ZH17) was used as wild type (WT), representing the genetic background of RNAi mutant lines. Eight rice seeds were germinated in a petri dish filled with moist tissue papers for 4–5 days then transferred to soil in 9 cm diameter plastic pots and placed in the greenhouses at 24 °C with 12-h light/dark cycle and 90% humidity. Three-week-old rice seedlings were used for gene expression analysis, AsA measurement, cell wall sugar composition analysis, transcriptome analysis and proteome analysis, whereas 2-month-old rice plants were used for anatomical observation. Moreover, the AsA contents in whole leaf and different parts of the leaf in RNAi lines were measured. Each leaf was equally divided into three parts: the top, middle and base.

For AsA measurement, eight rice seeds of three Thai rice varieties "Jao Hom Nin" (JHN), "Khaw Dok Mali 105" (KDML105) and "Gor Kor 6" (RD6) were germinated, grown in Yoshida nutrient solution [28] as modified by Gregorio et al. [29] and cultured in the greenhouse at 30 °C. The first and the second fully expanded leaves, stems and roots of three-week-old rice leaves were collected for AsA measurement. KDML105 was also used to determine the total AsA content in different growth stages including seed, seedling, 3-week-old, 12-week-old and 20-week-old plants. Leaves, stems and roots were separately collected, kept in liquid nitrogen and stored at −80 °C until measurement.

2.2. AsA Biosynthesis Gene Expression Analysis by Real-Time Quantitative PCR (qPCR)

Total RNA was extracted from 3-week-old leaf samples using an RNA extraction kit, according to the manufacturer's instructions (Vivantis, Selangor, Malaysia). Total RNA was reverse transcribed to cDNA using oligo (dT) primer and M-MLV reverse transcriptase (Promega, Madison, WI, USA). The cDNA was diluted to 1:20 dilution and used as a template for qPCR assay. The reaction was performed with the KAPA SYBR® FAST qPCR Master Mix (2X) (KAPA Biosystems, Wilmington, MA, USA). PCR was performed at 94 °C for 2 min followed by 35 cycles of 94 °C for 15 s, 58 °C for 15 s and 72 °C for 20 s for *OsActin* (Os03g0718100), *OSVTC1-1* (Os01g0847200), *OSVTC1-8* (Os08g0237200), *OsVTC4* (Os03g0587000), *OsGDH* (Os12g0482700) and *OsGPX1* genes (Os02g0664000). For *OsVTC1-3* (Os03g0268400), *OsGME1* (Os10g0417600), *OsGME2* (Os11g0591100) and *OsVTC2* (Os12g0190000) reactions were performed at 94 °C for 2 min followed by 35 cycles of 94 °C for 15 s, 55 °C for 15 s and 72 °C for 20 s. *OsActin* gene was used as a reference gene and the relative expression levels of each gene were calculated using the $2^{-\Delta\Delta CT}$ method [30]. The data were the mean of two biological replicates with three technical replicates for each sample. The primers used for qPCR were listed in Table 1.

Table 1. Primer sequences used for qPCR analysis.

Genes	Primer Sequence (5′-3′)	Product Size (bp)	Reference
OsVTC1-1	Forward: GTCATGTGAACTAACCCTCC Reverse: GAGTTTCTTCTGGTCCTCTTG	229	[8]
OsVTC1-3	Forward: CATCTCCAGCAGCATCATC Reverse: CATCGTCACCACCATGTAAAC	239	[8]
OsVTC1-8	Forward: GATTGTCATGTGAAATAATCC Reverse: CTCATTGAGAAGCAGTTATG	144	[8]
OsGME1	Forward: AGACTTCCACTGACAGGTTTG Reverse: TTCCAATGTTCACTGGCTCAC	132	[15]
OsGME2	Forward: GATGCCTATGGCTTGGAAAA Reverse: CAAAACGGTCAGTGGAGGTT	187	[31]
OsVTC2	Forward: GCAACCATCAACCACCTCCA Reverse: CACTATTCATTGTGCCCTCAGC	109	[15]
OsVTC4	Forward: GTTGGCCTTGAACATGTGTG Reverse: CCGAAGAATCAGAGCTCCAG	106	This study
OsGDH	Forward: AAGGGGAAAAACATTACAAAG Reverse: TTATCAATAGCGGAAGTAGACA	146	[15]
OsGPX1	Forward: GCTTACTGCATCACTTTGCC Reverse: GCAGTCGCAGGTCTCAATAA	76	[32]
OsActin	Forward: TCCATCTTGGCATCTCTCA Reverse: GTACCCTCATCAGGCATCTG	337	[33]

2.3. AsA Content Measurement

Samples (approximately 50 mg fresh weight) were homogenized using a Qiagen TissueLyser with two 3-mm steel beads for 30 s at 30 Hz, turned the blocks around and ground for another 30 s. Samples were added with 1 mL of cold 3% metaphosphoric acid (w/v) and centrifuged at 12,000× g, 4 °C for 10 min; 20 µL of supernatants and AsA standards (0.1–1.0 mM) were transferred to a 96-well UV-transparent microplate and added 2 µL of 10 mM Tris (2-carboxyethyl) phosphine. The microplate was incubated at room temperature for 10 min. Then, 100 µL of 0.2 M pH 7.0 phosphate buffer was added to the microplate, and the absorbance at 265 or 280 nm was recorded. After that, 5 µL ascorbate oxidase (40 units mL^{-1}) was added to the microplate and incubated at room temperature for 10 min. Finally, the absorbance was recorded again. The AsA concentration was calculated from the standard curve. Each experiment was repeated three times.

Another method to measure AsA in Thai rice varieties is described as follows. AsA content measurement was performed as previously described [34]. Samples were ground in liquid nitrogen into a fine powder of approximately 40 mg; 500 µL of 6% Trichloroacetic acid (TCA) (w/v) was added to a 1.5 mL microcentrifuge tube. Samples were centrifuged at 13,000× g, 4 °C for 10 min; 100 µL of supernatants were transferred to new microcentrifuge tubes and kept on ice. Then, 50 µL of 75 mM pH 7.0 phosphate buffer was added to 6% TCA (w/v) (blank), AsA standards (0.1–1.0 mM) and samples; 50 µL of 10 mM DTT was added to all assay tubes and incubated at room temperature for 15 min, and 50 µL of 0.5% NEM (w/v) was added to remove excess dithiothreitol (DTT) and incubated at room temperature for at least 30 s. Then, 250 µL of 10% TCA (w/v), 200 µL of 43% H_3PO_4 (v/v), 200 µL of 4% 2,2′-bipyridyl (w/v) and 100 µL of 3% $FeCl_3$ (w/v) were added to all assay tubes and incubated at 37 °C for 1 h. Finally, all assay tubes were measured for absorbance by spectrophotometer at 525 nm. AsA concentration was calculated from the standard curve.

2.4. Anatomical Observation of Leaves

Leaf samples of the 2-month-old wild type and *OsVTC1-1* RNAi lines were collected and cut into 0.5 cm sections. Samples were fixed in 50% formalin-acetic acid alcohol (FAAII) (*v*/*v*) fixative for 12 h, washed three times with 50% ethanol (*v*/*v*) for 3 h each and dehydrated with a tertiary butyl alcohol series (TBA) (50%, 70%, 85%, 95% and 100%) (*v*/*v*) for 12 h each. The dehydrated samples were infiltrated and embedded in histoplasts (Leica Biosystems, Wetzlar, Germany). The paraffin blocks were cut into sections 15 µm thick using a HistoCore BIOCUT manual rotary microtome (Leica Biosystems, Wetzlar, Germany). Sections were stained with Safranin and Fast green [35]. Photographs were taken using a Leica DM6 B light microscope equipped with a Leica DMC6200 digital camera (Leica Microsystems, Wetzlar, Germany). Ten random sites were photographed in three separate sections. The anatomical data were measured using ImageJ software version 1.53k (Wayne Rasband, National Institutes of Health, Bethesda, MD, USA).

2.5. Cell Wall Sugar Composition Analysis

2.5.1. Cell Wall Preparation

Leaf samples of 3-week-old wild type and *OsVTC1-1* RNAi lines, approximately 25 mg, were collected. Leaf samples were snap-frozen in liquid nitrogen and then ground to a fine powder using a Qiagen TissueLyser, as described previously. Plant cell wall preparation was performed using alcohol-insoluble residue (AIR) preparation method according to Conklin et al. [36]. Following this step, ice-cold 80% ethanol (*v*/*v*) was added to samples. Then, centrifugation at 12,000× *g* for 2 min was used to collect insoluble material. The supernatant was discarded and washed three times with 80% ethanol (*v*/*v*). Oligosaccharides associated with glycoprotein and polysaccharides in samples were hydrolyzed with 2 M trifluoroacetic acid (TFA) at 110 °C for 1 h. Non-hydrolyzed component was eliminated by centrifugation at 12,000× *g* for 2 min. The supernatant was evaporated to remove TFA. After hydrolysis, dried samples were added with myo-inositol (5 µM final concentration) and derivatized using methoxyamine hydrochloride dissolved in pyridine, followed by N-Methyl-N-(trimethylsilyl)trifluoroacetamide (MSTFA) (Sigma-Aldrich, St. Louis, MO, USA).

A 25 µM standard mix was prepared to contain D-glucose, D-galactose, D-mannose, D-xylose, D-arabinose, L-fucose, L-rhamnose, D-galacturonic acid, D-glucuronic acid, ribitol and Myo-inositol. This was diluted by half 6 times to a final concentration of 0.39 µM, to produce a calibration curve.

2.5.2. GC-MS Analysis and Data Analysis

The soluble monosaccharide compositions of cell wall samples were analyzed using an Agilent 7200 series-accurate mass Q-TOF GC-MS together with a 7890A GC system (Agilent Technologies, Santa Clara, CA, USA), equipped with an EI (electron ionization) ion source; 0.6 µL of each sample was injected into a non-deactivated, baffled glass liner with a 12:1 split ratio (14.448 mL min^{-1} split flow) and the inlet temperature was maintained at 250 °C. A Zebron semi-volatile (Phenomenex, Torrance, CA, USA) column (30 m × 250 µm × 0.25 µm), with a 10 m guard column, was maintained at a constant helium flow of 1.2 mL min^{-1}. The temperature gradient of the GC was ramped up at a rate of 15 °C min^{-1}, from 70 °C to 310 °C, over 16 min, and then held at 310 °C for a further 6 min. The total run time of 22 min was followed by a 7 min backflush at 310 °C to clean the column at the end of every run. The MS emission current and emission voltage were held at 35 µA and 70 eV, respectively, and the MS was automatically calibrated after every run. The mass range was set from 50 to 600 amu, with an acquisition rate of 5 spectra s^{-1}, and a solvent delay of 3.5 min.

Data were analyzed using Agilent technologies MassHunter qualitative version B.07.00 and quantitative software version B.08.00 (Agilent Technologies, Santa Clara, CA, USA). Samples were normalized to dry weight and the internal standard, Myo-inositol. Concentrations were calculated from the standard mix calibration curve.

2.6. Transcriptome Analysis

Leaf samples of wild type and *OsVTC1-1* RNAi lines were collected and used for RNA extraction by using the GF-1 Total RNA extraction kit (Vivantis, Malaysia). RNA samples were shipped for RNA sequencing (Novogene Bioinformatics Technology Co., Ltd., Beijing, China). Sample integrity was assayed on the Agilent 2100 Bioanalyzer (Agilent Technologies, Santa Clara, CA, USA). Library construction and RNA sequencing were pair-end sequenced by Novogene Bioinformatics Technology Co., Ltd., Beijing, China using Illumina Novaseq 6000 platform (Illumina, San Diego, CA, USA).

For data analysis of Illumina sequencing, the quality of the RNA-seq raw data was evaluated using FastQC 0.11.5 (multi-file) app in the CyVerse Discovery Environment (DE) [37]. Low-quality raw reads were removed by Trimmomatic. Then, the clean reads were mapped to the International rice genome sequencing project-1.0 (IRGSP-1.0) using TopHat v2.1.1. To identify the differentially expressed genes (DEGs) between WT and *OsVTC1-1* RNAi lines, we used Cuffdiff v.2.2.1 with a false discovery rate (FDR) less than 0.05 [37,38]. The value of Log2FC were used to determine significant differences in gene expression with log2FC > 1 (upregulated genes) or log2FC < −1 (downregulated genes). Gene descriptions of rice DEGs were identified using Gramene (http://www.gramene.org) (accessed on 11 March 2022). Heat map for differential gene expressions was performed using GraphPad Prism version 9.0.0 for Windows (San Diego, CA, USA).

2.7. Proteome Analysis

2.7.1. Protein Extraction

Leaf samples of wild type and *OsVTC1-1* RNAi lines were individually ground into powder in a mortar with liquid nitrogen. A total of 0.2 g of powder samples was dissolved in 0.5% SDS (*w*/*v*), and then placed in a continuous vortex for 3 h at room temperature. Samples were centrifuged at 8000 rpm for 10 min at room temperature. The supernatant was transferred at a new 1.5 mL centrifuge tube and subsequently mixed with 72% TCA (*w*/*v*), and 0.15% deoxycholate (*w*/*v*) was added to the samples and vortexed vigorously before placing samples overnight at −20 °C. The mixture was precipitated by centrifugation at 10,000 rpm for 10 min at room temperature and the pellets were washed with cold acetone until the pellet became white. The pellets were resuspended again in 0.5% SDS (*w*/*v*). Protein concentration was determined with the Lowry method [39].

2.7.2. Protein Digestion

Protein samples were subjected to in-gel digestion. Samples were completely dissolved in 10 mM ammonium bicarbonate (AMBIC), reduced disulfide bonds using 5 mM dithiothreitol (DTT) in 10 mM AMBIC at 60 °C for 1 h and alkylation of sulfhydryl groups by using 15 mM Iodoacetamide in 10 mM AMBIC at room temperature for 45 min in the dark. For digestion, samples were mixed with 50 ng/µL of sequencing grade trypsin (1:20 ratio) (Promega, Madison, WI, USA) and incubated at 37 °C overnight. Prior to LC-MS/MS analysis, the digested samples must be dried and protonated with 0.1% formic acid (*v*/*v*) before injection into LC-MS/MS.

2.7.3. Liquid Chromatography-Tandem Mass Spectrometry (LC-MS/MS)

The tryptic peptide samples were prepared for injection into an Ultimate3000 Nano/Capillary LC System (Thermo Fisher Scientific, Waltham, MA USA) coupled to a Hybrid quadrupole Q-Tof impact II™ (Bruker Daltonics GmbH, Bremen, Germany) equipped with a Nano-captive spray ion source. Briefly, peptides were enriched on a µ-Precolumn 300 µm i.d. × 5 mm C18 Pepmap 100, 5 µm, 100 A (Thermo Fisher Scientific, Waltham, MA USA), separated on a 75 µm I.D. × 15 cm and packed with Acclaim PepMap RSLC C18, 2 µm, 100 Å, nanoViper (Thermo Fisher Scientific, Waltham, MA USA). Solvents A and B containing 0.1% formic acid (*v*/*v*) in water and 0.1% formic acid (*v*/*v*) in 80% acetonitrile (*v*/*v*), respectively were supplied on the analytical column. A gradient of 5–55% solvent B was used to elute the peptides at a constant flow rate of 0.30 µL/min for 30 min.

Electrospray ionization was carried out at 1.6 kV using the CaptiveSpray (Bruker Daltonics GmbH, Bremen, Germany). Mass spectra (MS) and MS/MS spectra were obtained in the positive-ion mode over the range (m/z) 150-2200 (Compass 1.9 software, Bruker Daltonics GmbH, Bremen, Germany).

2.7.4. Protein Identification

The analyzed MS/MS data from LC-MS were measured for peptide MS signal intensities by MaxQuant version 1.6.6.0 (Max-Planck Institute for Biochemistry, Martinsried, Germany), including the in-built andromeda search engine for label-free quantification [40]. The data were searched against the Uniprot database (released date 26 January 2022) for protein identification. Database interrogation was taxonomy (*Oryza sativa*); enzyme (trypsin); variable modifications (carbamidomethyl, oxidation of methionine residues); mass values (monoisotopic); protein mass (unrestricted); peptide mass tolerance (1.2 Da); fragment mass tolerance (±0.6 Da), peptide charge state (1+, 2+ and 3+) and max missed cleavages. The identified protein was analyzed with the MultiExperiment Viewer software (MeV, version 4.9.0, J. Craig Venter Institute, La Jolla, CA, USA) and filtered with a one-way ANOVA ($p < 0.05$) [41]. Uniprot (http://www.uniprot.ort/) (accessed on 26 January 2022) and search tools were used to identify gene ontology (GO). For visualizing, the overlapped proteins were generated by Venny v2.1.0 (https://bioinfogp.cnb.csic.es/tools/venny/) (accessed on 17 March 2022).

2.8. Statistical Analysis

All data are presented as mean ± SE. The qPCR experiment was repeated at two biological replicates (three technical replicates for each biological replicate). The AsA content and sugar composition experiments were repeated three times. Statistical analyses were performed using IBM SPSS Statistics v. 26 software (IBM, New York, NY, USA). The data were performed using Student's *t*-test or one-way ANOVA followed by a Tukey's HSD post-hoc test to determine statistical significance. Heat map of the fragments per kilobase of transcript per million fragments (FPKM) value was generated using GraphPad Prism version 9.0.0 for Windows (GraphPad Software, San Diego, CA, USA) to evaluate the similarity among three replicates. The principal component analysis (PCA) was also performed using FPKM values generated by factoextra package in RStudio [42].

3. Results

3.1. Gene Expression Analysis by Quantitative Real-Time PCR (qRT-PCR)

The transcript levels of genes in the ascorbic biosynthesis pathway including three copies of *GDP-mannose pyrophosphorylase* (*VTC1*), namely *OsVTC1-1*, *OsVTC1-3* and *OsVTC1-8*, two copies of *GDP-mannose-3′,5′-epimerase* (*GME*), *OsGME1* and *OsGME2*, *GDP-L-galactose phosphorylase* (*OsVTC2*), *L-galactose-1-phosphate phosphatase* (*OsVTC4*), *L-galactose dehydrogenase* (*OsGDH*) and *glutathione peroxidase* (*OsGPX1*) genes were examined. The mRNA expression levels of *OsVTC1-1*, *OsGME1*, *OsGME2*, *OsVTC2* and *OsGPX1* genes were statistically significantly lower in RNAi mutant lines compared to the expression level in wild type (Figure 1a,d–f,i). The expression levels of *OsVTC1-3*, *OsVTC1-8* and *OsVTC4* genes were not different from the wild type (Figure 1b,c,g). However, the transcript levels of *OsGDH* genes were statistically significantly higher in RNAi mutant lines compared to wild type (Figure 1h). The results revealed that the reduction of *OsVTC1-1* gene expression influenced the expression level of genes in the ascorbic biosynthesis pathway and *OsGPX1*.

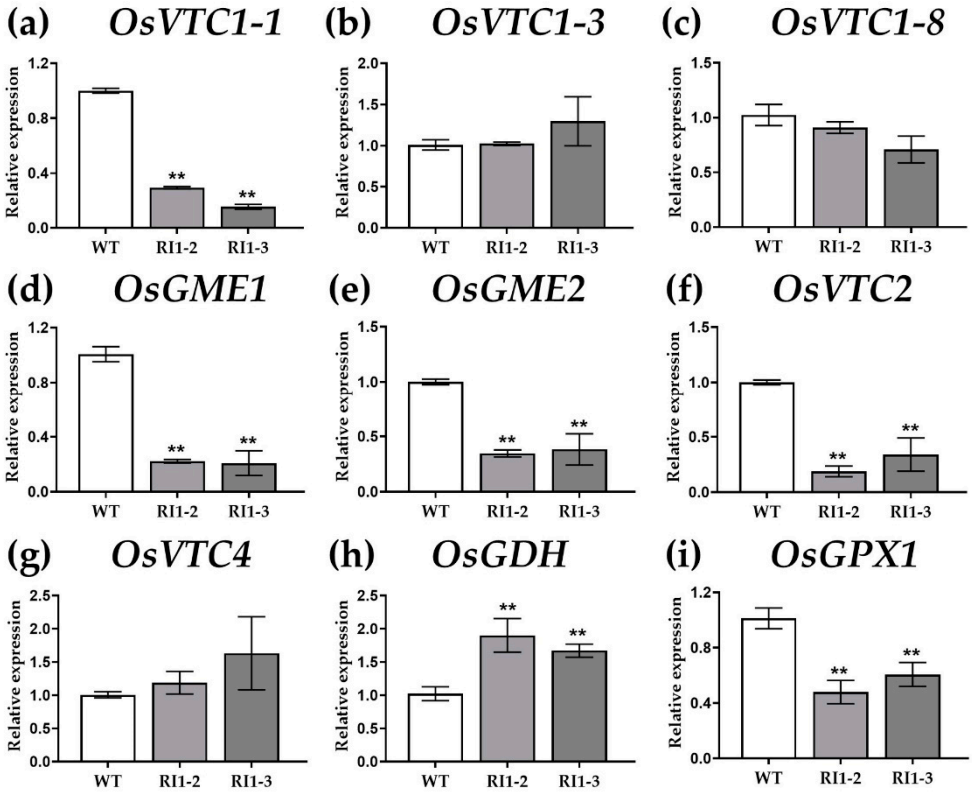

Figure 1. qPCR analysis of genes related in AsA biosynthesis pathway and antioxidant enzyme are shown as follows: (**a**) *OsVTC1-1*; (**b**) *OsVTC1-3*; (**c**) *OsVTC1-8*; (**d**) *OsGME1*; (**e**) *OsGME2*; (**f**) *OsVTC2*; (**g**) *OsVTC4*; (**h**) *OsGDH*; (**i**) *OsGPX1* genes. Bars represent the means and standard errors of two biological replicates (three technical replicates per biological replicate). Asterisk indicates statistically significant differences from Zhonghua17 (wild type) analyzed using Student's *t*-test (** $p < 0.01$).

3.2. AsA Measurement

To compare AsA content between wild type and *OsVTC1* RNAi lines, we measured the amount of AsA in whole leaves. The AsA production was significantly reduced by ~34 and 40% in RI1-2 and RI1-3 lines compared to wild type (Figure 2a). The three different parts of fully expanded leaves referred to as top, middle and base areas were also measured for AsA content. The results revealed that the top part of the leaves contained the highest amount of AsA, followed by the middle and the base of the leaves. Moreover, the amount of AsA in the wild type was significantly higher than that in the mutant lines in the top part of leaves, but not different in the middle part and base of leaves, respectively (Figure 2b).

In addition, we measured the AsA contents in leaves, stems and roots of three different Thai rice cultivars (KDML105, JHN and RD6) and measured the AsA contents of KDML105 rice cultivar at different rice growth stages (seed, seedling, 3 weeks-old, 12 weeks-old and 20 weeks-old plants) in leaves, stems and roots. The results showed that the AsA content was not different in three Thai rice cultivars, but the AsA contents were significantly higher in leaves than in stems and roots (Figure 2c). The AsA was not detected in the seed and seedling stage. On the other hand, the AsA was detected at a 3-week-old plant at a relatively high level and stayed at this high level at 12- and 20-week-old plants, in which the highest amount was detected in leaves (Figure 2d).

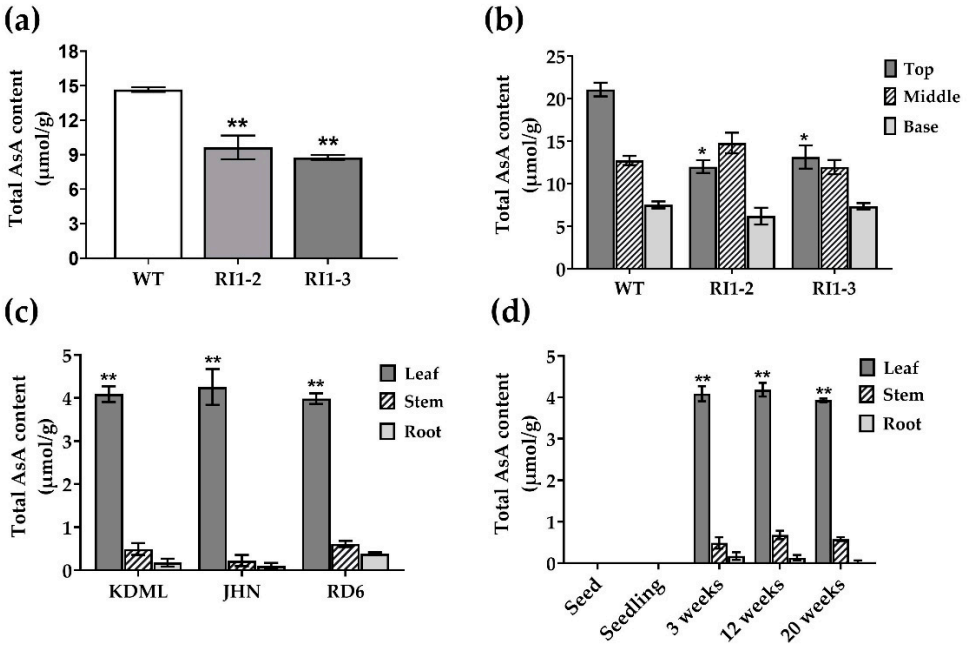

Figure 2. Measurement of the total AsA content in the wild type and RNAi lines, Thai rice cultivars and growth stages. (**a**) The total AsA content in the wild type and RNAi lines in whole leaf; (**b**) in different parts of leaves including top, middle and base; (**c**) The total AsA content in KDML, JHN and RD6 in leaves, stems and roots; (**d**) The total AsA content in KDML in different growth stages including; seed, seedling, 3 weeks, 12 weeks and 20 weeks old in leaves, stems and roots. Bars represent the means and standard errors of three replicates. (**a**) Asterisk indicates statistically significant differences from Zhonghua17 (wild type) analyzed using Student's *t*-test. (**b**) Asterisk indicates statistically significant differences from wild type in each leave areas analyzed using Student's *t*-test. (**c**,**d**) Asterisk indicates statistically significant differences from roots analyzed by one-way ANOVA with Tukey's HSD test (* $p < 0.05$ and ** $p < 0.01$).

3.3. Leaf Anatomical Comparison between Wild Type and OsVTC1-1 RNAi Lines

OsVTC1-1 RNAi lines were observed through cross-sections of flag leaves to compare cell size and tissue organization with the wild type (Figure 3a–c). The results revealed that parenchyma thickness, the thickness of large vascular bundle (LVB) and small vascular bundle (SVB), the distance between adjacent SVBs, the thickness of upper and lower cuticle and thickness of upper epidermis of *OsVTC1-1* RNAi lines were significantly lower than in wild type (Figure 3d–g,i–k). However, there was no significant difference in the length of the largest bulliform cell and thickness of the lower epidermis between *OsVTC1-1* RNAi lines and wild type (Figure 3h,l). Therefore, the limitation of *OsVTC1-1* expression in leaves might affect cell size and tissue arrangement in leaves.

3.4. Cell Wall Sugar Composition Analysis

To investigate whether *OsVTC1-1* gene is involved in the cell wall modification mechanism, we compared cell wall monosaccharide composition in wild type (WT) and *OsVTC1-1* RNAi lines. Xylose, arabinose, galactose, galacturonic acid, fucose, mannose and glucuronic acid were detected in hydrolyzed cell wall samples. There was not a statistically significant difference in monosaccharide composition (µmol g^{-1} FW) from RNAi lines compared to the WT (Figure S1). Xylose is the most abundant monosaccharide, followed by arabinose and galactose (Figure S1a–c). However, galactose and mannose contents as mol% of the total acid-hydrolyzed sugars were significantly decreased in both RI1-2 and RI1-3 lines (Figure 4c,f). These data revealed that reduction of *OsVTC1-1* gene expression affects sugar incorporation into the cell wall, especially galactose and mannose.

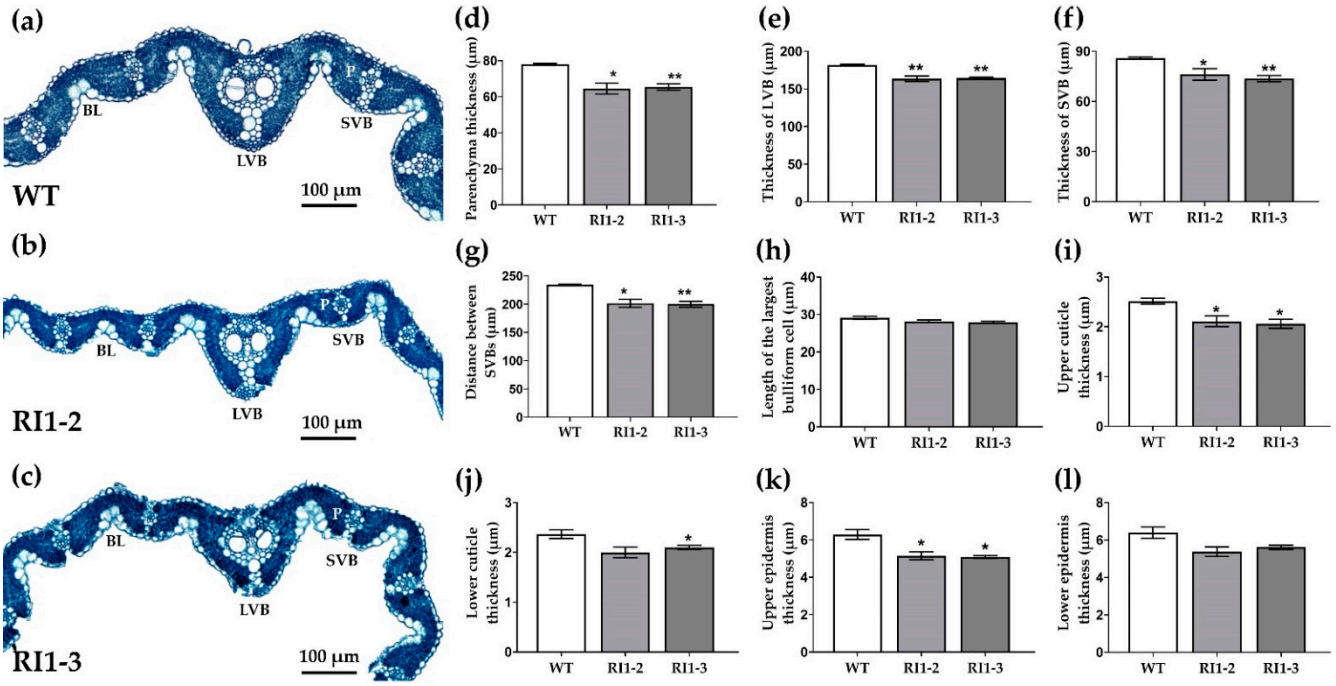

Figure 3. Leaf anatomical features of wild type (WT) and *OsVTC1-1* RNAi lines. (**a**) Transverse paraffin sections of leaves from WT; (**b**) RI1-2 line; (**c**) RI1-3 line. (**d**) Parenchyma thickness; (**e**) Thickness of large vascular bundle (LVB); (**f**) Thickness of small vascular bundle (SVB); (**g**) Distance between adjacent SVBs; (**h**) Length of the largest bulliform cell; (**i**) Upper cuticle thickness; (**j**) Lower cuticle thickness; (**k**) Upper epidermis thickness; (**l**) Lower epidermis thickness. BL, bulliform cells; LVB, large vascular bundle; P (white color), parenchyma; SVB, small vascular bundle. Bars represent the means and standard errors of three replicates. Asterisk indicates statistically significant differences from wild type analyzed using Student's *t*-test (* $p < 0.05$, ** $p < 0.01$).

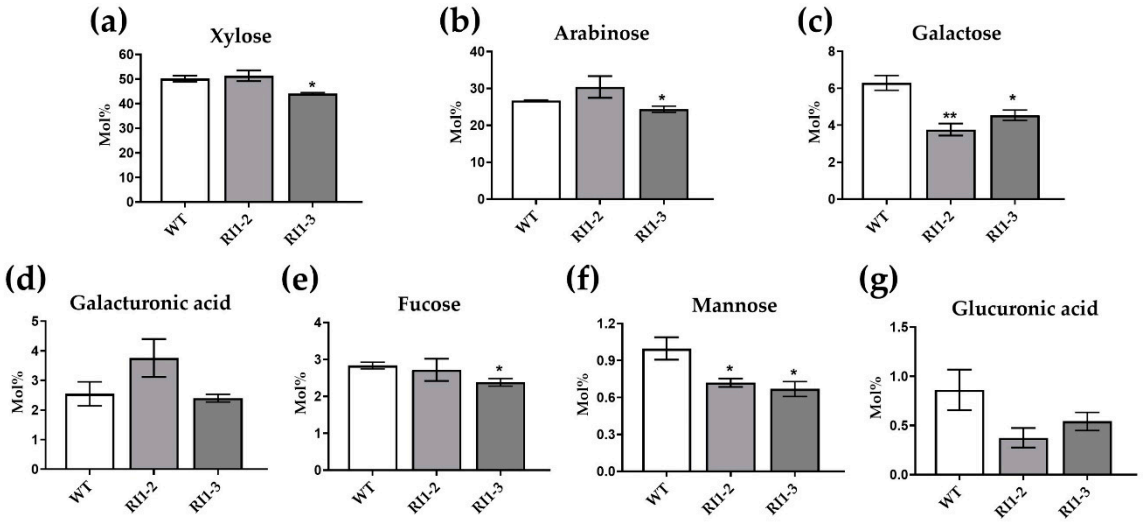

Figure 4. Cell wall monosaccharide composition (mol%) isolated from 3-week-old wild type (WT) and *OsVTC1-1* RNAi lines. (**a**) xylose; (**b**) arabinose; (**c**) galactose; (**d**) galacturonic acid; (**e**) fucose; (**f**) mannose; (**g**) glucuronic acid. Bars represent the means and standard errors of three replicates. Asterisk indicates statistically significant differences between WT and *OsVTC1-1* RNAi lines analyzed using Student's *t*-test (* $p < 0.05$ and ** $p < 0.01$).

3.5. Transcriptome Analysis

We performed transcriptome analysis to identify differentially expressed genes (DEGs) between wild type (WT) and *OsVTC1-1* RNAi lines. The RNA-seq data revealed that the raw reads and clean reads in each sample ranging from 39,859,454 to 43,623,072 reads and 19,704,679 to 23,321,544, respectively. The total mapped reads varied between 90.7% and 93.0% (Table S1). There were 25 and 19 down-regulated DEGs in RI1-2 and RI1-3, respectively. The down-regulated DEGs in RI1-2 and RI1-3 are listed in Table 2. Eleven down-regulated genes were common between RI1-2 and RI1-3 including *thionin-like peptide*, *aspartokinase*, *aspartokinase/homoserine dehydrogenase 2*, *CBL-interacting protein kinase 14* (*CIPK14*), *ARK protein*, *kinase*, *pheophorbide an oxygenase* and *photosystem II 10 kDa polypeptide*. There were 100 and 256 up-regulated DEGs in RI1-2 and RI1-3, respectively. A list of the top 20 DEGs ranked by the log2FC value is listed in Table S2. *F-box protein*, *jasmonate-induced protein*, *amino acid transporter* and *glycosyl transferase* were found to be common in the top 20 up-regulated DEGs among RI1-2 and RI1-3 lines (Table S2). Heat map representing 100 common genes from WT and *OsVTC1-1* RNAi lines correspond to the fragments per kilobase of transcript per million fragments (FPKM) value was generated using GraphPad Prism version 9.0.0 to evaluate the similarity among three replicates. The results showed that the expression profiles of most genes were similar among three replicates (Figure S2, Table S3). The principal component analysis (PCA) was also performed using FPKM values. PCA plots declared that the WT samples were grouped together, whereas six replicates of *OsVTC1-1* RNAi lines were also clustered together with two replicates (RI1-2_3 and RI1-3_3) spaced a bit further apart (Figure S3).

Table 2. Downregulated differentially expressed genes in RI1-2 and RI1-3 as ranked by log2FC value.

Downregulated DEGs of RI1-2			
No.	**Gene ID**	**Gene Description**	**Log2FC**
1	OS07G0677200	Peroxidase	−5.186
2	OS07G0432201	Similar to thionin-like peptide	−4.666
3	OS02G0139500	Similar to beta-amyrin synthase	−3.203
4	OS12G0583300	Peptidase aspartic, catalytic domain containing protein	−3.163
5	OS03G0850400	Similar to aspartokinase	−3.157
6	OS09G0294000	Similar to bifunctional aspartokinase/homoserine dehydrogenase 2,chloroplast precursor	−2.759
7	OS10G0562900	Non-protein coding transcript	−2.656
8	OS01G0791033	Similar to ribulose-1,5-bisphosphate carboxylase/oxygenase large subunit	−2.433
9	OS12G0628600	Similar to thaumatin-like pathogenesis-related protein 3 precursor	−2.352
10	OS03G0355300	Protein of unknown function DUF1618 domain containing protein	−2.136
11	OS09G0541600	Conserved hypothetical protein	−2.089
12	OS12G0113500	Similar to CBL-interacting protein kinase 14	−2.045
13	OS01G0117200	OsRLCK16 Similar to ARK protein (Fragment)	−1.984
14	OS07G0475900	Similar to kinase family protein	−1.951
15	OS06G0581500	Protein kinase, core domain containing protein	−1.801
16	OS12G0141400	Conserved hypothetical protein	−1.761
17	OS12G0428000	Similar to senescence-associated protein DIN1	−1.753
18	OS03G0805600	Similar to pheophorbide *a* oxygenase	−1.514
19	OS07G0109700	Conserved hypothetical protein	−1.421
20	OS07G0147500	Similar to Photosystem II 10 kDa polypeptide, chloroplast precursor	−1.341
21	OS01G0762300	Similar to predicted protein	−1.340
22	OS02G0202200	SPX domain-containing protein	−1.270
23	OS08G0117200	Similar to 40S ribosomal protein S13 (Fragment)	−1.246
24	OS10G0465800	Similar to 60S ribosomal protein L21	−1.229
25	OS01G0949300	EF-Hand type domain containing protein	−1.113

Table 2. *Cont.*

Downregulated DEGs of RI1-3			
No.	**Gene ID**	**Gene Description**	**Log2FC**
1	OS07G0432201	Similar to thionin-like peptide	−4.554
2	OS09G0294000	Similar to bifunctional aspartokinase/homoserine dehydrogenase 2, chloroplast precursor	−2.996
3	OS03G0850400	Similar to aspartokinase	−2.696
4	OS06G0685300	Similar to predicted protein	−2.668
5	OS11G0416900	ABC transporter-like domain containing protein	−2.440
6	OS12G0113500	Similar to CBL-interacting protein kinase 14	−2.434
7	OS01G0117200	Similar to ARK protein (Fragment)	−2.182
8	OS01G0162200	Leucine-rich repeat domain containing protein	−2.123
9	OS07G0475900	Similar to kinase family protein	−2.089
10	OS08G0100300	Non-protein coding transcript	−1.966
11	OS07G0691200	Similar to D-alanine–D-alanine ligase B	−1.901
12	OS06G0581500	Protein kinase, core domain containing protein	−1.758
13	OS12G0141400	Conserved hypothetical protein	−1.745
14	OS07G0663800	Similar to oxidoreductase	−1.662
15	OS01G0762300	Similar to predicted protein	−1.584
16	OS07G0147500	Similar to Photosystem II 10 kDa polypeptide, chloroplast precursor	−1.431
17	OS10G0396300	Similar to MOB1 MOB Kinase Activator 1A	−1.357
18	OS02G0814400	Cytochrome c, monohaem domain containing protein	−1.275
19	OS03G0805600	Similar to pheophorbide a oxygenase	−1.244

3.6. Proteome Analysis

To identify differentially expressed proteins between wild type (WT) and *OsVTC1-1* RNAi lines, we used liquid chromatography-tandem mass spectrometry (LC/MS-MS) to analyze peptide sequences. The peptide sequences data were searched using Uniprot (http://www.uniprot.ort/) (accessed on 26 January 2022). From an overall 115 proteins, 44, 85 and 86 were found in wild type, RI1-2 and RI1-3 lines, respectively, while 7, 8 and 6 proteins were uniquely observed in wild type, RI1-2 and RI1-3 lines, respectively. Six proteins were common in all samples (Figure 5). The differentially expressed proteins are shown in Table 3. Seven proteins were particularly found in wild type, including protein disulfide isomerase-like 1-1, anoctamin-like protein, minor outer capsid protein P2, peroxisomal fatty acid beta-oxidation multifunctional protein, mitogen-activated protein kinase, mixed-linked glucan synthase 6 and DNA topoisomerase 3-alpha. In addition, the NAC domain-containing protein 50, very-long-chain aldehyde decarbonylase, 2-hydroxyacyl-CoA lyase, kinesin-like protein KIN-13A, cysteine-tRNA ligase, double-stranded RNA-binding protein 6, zinc finger CCCH domain-containing protein 15 and endoribonuclease dicer homolog 1 were presented only in RI1-2 and RI1-3 lines. Some differentially expressed proteins are known to play a role in the cell wall structure. For example, kinesin-like protein KIN-4A, expansin-B2, beta-galactosidase 11 and cellulose synthase-like protein D5 were more abundant in wild type than in the RI1-2 line (Table 3).

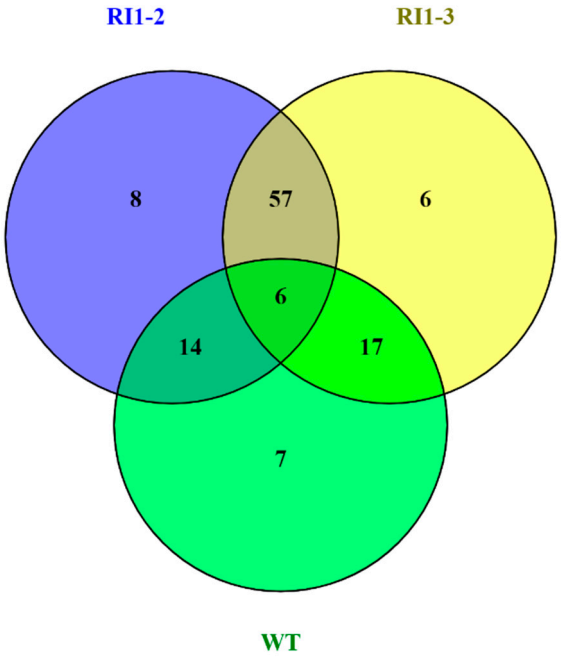

Figure 5. Venn diagram of wild type (green) proteome overlapped with RI1-2 (blue) and RI1-3 (yellow) lines.

Table 3. Differentially expressed proteins in WT and *OsVTC1-1* RNAi lines.

Protein ID	Protein Name	Peptide Sequence	Log2 Protein Abundance		
			WT	RI1-2	RI1-3
Q53LQ0	Protein disulfide isomerase-like 1-1	FLIGDIEASQGAFQYFGLREDQ VPLIIIQDGESKK	15.67	0	0
Q0JJZ6	Anoctamin-like protein	LSAPMGTLGR	14.95	0	0
O56834	Minor outer capsid protein P2	NLFSLLQKRK	13.89	0	0
Q8W1L6	Peroxisomal fatty acid beta-oxidation multifunctional protein	MNKAMSLLKGALDYSDFK	13.66	0	0
Q5QN75	Mitogen-activated protein kinase	RGKKPHK	13.59	0	0
Q84UP7	Mixed-linked glucan synthase 6	SHPYMGRAQEEFVNDRR	12.38	0	0
C7J0A2	DNA topoisomerase 3-alpha	ASRYFRMSSEHTMK	12.03	0	0
Q9SQX9	NAC domain containing protein 50	NASGQAS	0	14.88	14.80
Q6ETL8	Very-long-chain aldehyde decarbonylase	LAAMRLPK	0	13.19	13.43
Q0JMH0	2-hydroxyacyl-CoA lyase	ARDNVLKMEAQLAK	0	15.58	15.05
B9FMJ3	Kinesin-like protein KIN-13A	LARFQHRLK	0	13.85	14.66
Q0IZQ2	Cysteine-tRNA ligase	QYEKSDEIR	0	12.47	14.73
Q9AV50	Double-stranded RNA-binding protein 6	ILPLFRPKSNSR	0	16.49	14.17
Q6K4V3	Zinc finger CCCH domain-containing protein 15	APSSTSK	0	15.22	14.92
Q9SP32	Endoribonuclease dicer homolog 1	AEENKSKPEER	0	14.70	14.53
Q7FAD5	Synaptonemal complex protein ZEP1	ARLLYVDSRLECMEQELK	12.49	15.82	15.43
Q6ZCZ2	Brassinosteroid LRR receptor kinase BRL3	NFARQSVFLAVTLSVLILF SLLIIHYKLWK	11.70	14.56	14.02
Q0DV66	Pheophorbide a oxygenase	AWWQLVPR	14.21	14.26	12.17
Q0D5P3	Formin-like protein 11	EASKVAPVK	11.62	14.11	14.05
Q7XD96	Endoribonuclease	ASLCLHMSYFK	12.20	13.78	14.07
Q67W65	Transcription initiation factor TFIID subunit 1	EDELQKAK	13.86	12.72	13.59
Q6YUL8	Kinesin-like protein KIN-4A	ARNIQNKPIVNR	14.76	0	11.32

Table 3. *Cont.*

Protein ID	Protein Name	Peptide Sequence	Log2 Protein Abundance		
			WT	RI1-2	RI1-3
O24230	Expansin-B2	MAGASAK	14.52	0	14.70
Q6ZJJ0	Beta-galactosidase 11	DLHHALR	13.7	13.2	0
Q2QNS6	Cellulose synthase-like protein D4	LLIAIRLVALGFFLAWRIR	12.93	13.19	0
Q5Z6E5	Cellulose synthase-like protein D5	ICYIQFPQRFEGIDPSDR	10.74	0	13.02

4. Discussion

AsA biosynthesis in plants predominantly involves the conversion of D-glucose-6-phosphate to AsA via GDP-mannose and GDP-L-galactose [5]. Evidence for the importance of the L-galactose pathway in AsA production has been studied in several mutants. Many studies showed that the mutants affected the AsA levels, plant growth and development and abiotic stress tolerance. *vtc1* mutant, which is a knock-down mutant of *GDP-mannose pyrophosphorylase* (*VTC1*) gene, contained 25% AsA levels compared to wild type [7]. Mutants in *VTC2* (*vtc2-1* and *vtc2-2*), which encodes GDP-L-galactose phosphorylase, contain ~20% of wild type AsA and are sensitive to ozone in Arabidopsis [43]. Similarly, the AsA content and seed germination rate in Arabidopsis was decreased in the T-DNA knockout *vtc4* mutant (*L-galactose-1-phosphate phosphatase*). Although the L-galactose pathway was controlled by several genes, *VTC*2 gene was identified as the first rate-limiting step of the L-galactose pathway [14]. However, *VTC1* gene is also required for ascorbate production in plants. For example, the AsA production of whole rice plants reduced ~30–60% in *OsVTC1-1* RNAi lines and decreased salt tolerance under salt stress [8,11]. In potatoes, antisense down-regulation of *VTC1* gene reduced AsA content and GMPase activity [44]. Overexpression of *GMP* or *VTC1* gene increases the GMPase activity and leads to a two- to four-fold increase in the AsA content in leaves [45].

In this study, expression levels of eight genes in the L-galactose pathway and glutathione peroxidase (*OsGPX1*) gene in wild type and *OsVTC1-1* RNAi lines were examined. Our results showed that *OsVTC1-1* RNAi lines led to a reduced expression level of *OsVTC1-1* gene, but it did not affect the expression of *OsVTC1-3* and *OsVTC1-8* genes. This result is consistent with a previous study [8]. The mRNA transcript levels of *OsVTC1-1* and *OsVTC1-3* genes showed the highest expression in leaves and roots, respectively, while *OsVTC1-8* expression level was low in both leaves and roots. The transcript levels of *GDP-mannose-3′,5′-epimerase* (*OsGME1*, *OsGME2*) and *OsVTC2* also decreased in RNAi lines. There have been several studies on the mutation of AsA-related genes. *vtc1* mutant had decreased AsA to 70% of wild type levels in Arabidopsis [10]. Overexpression of *GMP* gene had resulted in higher AsA levels in several plants species, including 2.0-fold in tobacco [46], 1.3-fold in Arabidopsis [47] and 1.7-fold in tomato [48]. On the other hand, the AsA content of *GME* RNAi lines in tomatoes was decreased by 40–60% [49]. Similarly, AsA content in Arabidopsis *vtc2-4* and *vtc2-1* mutant lines was 70% lower than in wild type [50]. There was no effect on the expression of *L-galactose-1-phosphate phosphatase* (*OsVTC4*) and *L-galactose dehydrogenase* (*OsGDH*) genes. *VTC4* and *GDH*, which are downstream genes in the L-galactose pathway, are not a major rate-limiting step in the L-galactose pathway in rice. VTC4 has a wide substrate specificity and is involved in the synthesis of both myo-inositol and AsA [16]. In tomatoes, the AsA content was unchanged in *GPP* (*VTC4*) overexpression line [51]. The AsA concentration in leaves was not affected in *GDH* overexpression lines of tobacco, although the transgenic lines exhibited a 3.5-fold increase in GDH activity [52].

GPX gene expression also decreased in *OsVTC1-1* RNAi lines. GPX is an important enzymatic antioxidant to scavenge hydrogen peroxide (H_2O_2) and peroxide radicals against oxidative damage. AsA is involved in the detoxification of ROS either directly or through the ascorbate-glutathione (AsA-GSH) pathway [53,54]. Previously, Zhang et al. reported that a tomato ethylene response factor, also called TERF1, plays a role in regulating ROS

scavenging during stress responses. Overexpression of *TERF1* in tobacco increased the expression of the oxidative-related genes—not only the *GPX* gene that catalyzes oxidative reactions but also the *VTC1* gene in the AsA biosynthesis pathway. This finding suggests that the AsA and GPX coordinates function in the regulation of ROS detoxification. For this reason, decreasing the expression of *VTC1* gene could affect the transcript level of genes related to oxidative stress, such as *GPX* [55,56].

AsA, which is a multifunctional molecule that plays a significant role in plant growth and development, including enzymes, is involved in multiple biological processes, photosynthesis, ROS scavenging and tolerance against both abiotic and biotic stresses [1,5,57]. The rice genome consists of three homologs of *OsVTC1* gene. Among these homologs, *OsVTC1-1* is associated with the greatest AsA production in rice leaves, whereas *OsVTC1-3* plays a role in AsA synthesis in roots [8]. Our results were in agreement with a previous report [8]. The expression levels of genes in the L-galactose pathway in roots were quite low as compared to leaf levels, implying that rice synthesizes AsA mainly in leaves [15]. The amount of AsA was highest at the top and decreased down to the base of leaves. AsA is synthesized in all parts of leaves (and other parts of the plants). It has a concentration of more than 20 mM in chloroplasts [5]. This study showed that AsA accumulated more in the top of the leaves. It could possibly be related to higher light intensity because AsA acts as a photoprotectant during light exposure. Moreover, AsA acts as an electron donor in photosynthesis, while monodehydroascorbate acts as an electron acceptor [2]. It is involved in the removal of H_2O_2 generated by photoreduction and photorespiration [53]. Therefore, the AsA was accumulated in the area of plants that are exposed to higher light intensity. Supporting again in leaves contained a high amount of AsA but low in roots. Similarly, Shih et al. [58] showed that AsA activities of *Moringa oleifera*, Lam were high in leaves, followed by stems and stalks, respectively. The total AsA contents were the highest in flowering buds, then siliques and leaves, but low in stems [59]. In addition, the absence of AsA content was observed in seeds. To maintain metabolic activity at a low level, dry seed avoids its reduced form (AsA), and comprises only the oxidized form; dehydroascorbic acid (DHA) [60,61].

According to the comparative anatomical characteristics between *OsVTC1-1* RNAi lines and WT plants in rice under a light microscope, the results revealed that the leaf anatomical parameters were altered in *OsVTC1-1* RNAi lines. The decrease in size of parenchyma, large and small vascular bundles of RNAi lines reflect the roles of AsA in its photosynthetic tissue and vascular system. This is because leaf parenchyma generally contains abundant chloroplast, which is a source of high AsA accumulation [1,2]. In Arabidopsis, AsA was detected not only in parenchyma cells but also in xylem and phloem elements [62]. Moreover, AsA has been known to be required for vascular development at the different stages of xylem and phloem in larch (*Larix sibirica* Ldb.) and pine (*Pinus sylvestris* L.) trees [63]. In our study, the distance between adjacent small vascular bundle (SVBs) in *OsVTC1-1* RNAi lines was also shorter than wild type, suggesting that cell size reduction of both parenchyma and vascular tissue may affect the length between adjacent SVBs. This result was supported by the distance between two adjacent vascular bundles decreased due to the reduction of mesophyll and bundle sheath cell thickness in the presence of NaCl [64]. Similarly, the thickness of cuticle and epidermis of the upper surface and lower cuticle thickness in *OsVTC1-1* RNAi leaf was significantly smaller than in wild type. A previous study also showed that the cell size in *vtc1* and *vtc2* were smaller than wild type in Arabidopsis [9]. AsA is necessary for many biological processes in plants, including cell expansion, cell division and cross-linking of the cell walls [2,4]. Therefore, the reduction of AsA synthesis by knocking down *OsVTC1-1* gene expression likely disrupts the cell size and cellular organization in leaves.

VTC1 catalyzes the synthesis of GDP-D-mannose, which is a substrate for cell wall polysaccharide and glycoprotein synthesis, and likewise GDP-L-galactose [3]. In grasses, xylose is the major component of hemicellulose monosaccharide (about 60%) [65]. Our study showed that xylose is abundantly present in leaf cell walls in both WT and *OsVTC1*

RNAi lines. In addition, mannose and galactose composition as mole percentages of total sugars decreased in both RI1-2 and RI1-3 RNAi lines. Similar to a previous study in potato, the GMPase (VTC1) antisense plants exhibited a reduction in the mannose content of cell walls in leaves, while other monosaccharides content in cell walls were not different from the wild type. Reduction in the mannose content of cell walls in GMPase antisense plants was a result of a reduction in GDP-mannose production [44]. In the cell walls of Arabidopsis *vtc1* mutant, mannose and fucose levels were also decreased [66]. Decreasing *VTC1* expression led to a reduction in the mannose and galactose composition, suggesting that *VTC1* may be involved in cell wall formation because sugars are components of plant cell wall polymers [67]. Sugars play a role in plant development, as well as plant signaling pathways [68]. Consistent with anatomical results, *OsVTC1-1* RNAi lines showed a decrease in cell size. AsA is involved in the regulation of plant development processes, acts as a cofactor in cell wall hydroxyproline-rich glycoproteins post-translation for cell growth and is required for cell division [2,5].

Transcriptome analysis revealed DEGs between wild type and *OsVTC1-1* RNAi lines, and the 11 down-regulated differentially expressed genes (DEGs) were shared in both *OsVTC1-1* RNAi lines. Several DEGs are involved in the signaling pathways, such as aspartokinase, CBL-interacting protein kinase 14 (CIPK14) and kinase. Consistent with our results, a previous study reported that 171 genes were differentially expressed between wild type and *vtc1* mutants in Arabidopsis, including kinase and kinase receptors [69]. Aspartokinase catalyzes the phosphorylation of aspartic acid, which is the first step of amino acids synthesis, such as lysine, methionine and threonine [70]. Reduced aspartokinase activity in myxobacteria led to disruption of cell wall growth [71]. CIPK14 interacts with Calcineurin B-like (CBL) protein which responds to various abiotic stresses and associates with plant development [72]. In eukaryotic cells, kinases play a key role in cellular processes by adding phosphate groups and act as a major component which responds to abiotic and biotic stresses in plants [73]. Another identified DEG that involves in amino acids synthesis is aspartokinase/homoserine dehydrogenase 2. This enzyme is a bifunctional protein and catalyzes the synthesis of threonine, methionine and isoleucine [74]. The thionin-like peptide is a defense-related protein which has antimicrobial activity [75]. Some DEGs are associate with photosynthesis; pheophorbide an oxygenase controls chlorophyll breakdown during senescence, which is one part of plant development [76]; and photosystem II 10 kDa polypeptide is a chloroplast precursor in photosystem II [77]. Hence, decreasing *OsVTC1-1* expression may affect many processes in plants.

Differentially expressed proteins between wild type and *OsVTC1-1* RNAi lines were additionally determined. Cell wall-related proteins, including kinesin-like protein KIN-4A, expansin-B2, beta-galactosidase 11 and cellulose synthase-like protein D5 were reduced in mutant lines compared with wild type. Several studies on the mutation of cell wall-related genes have been reported. For example, the expansion of cells is accomplished through the activity of expansin as a cell wall protein [78]. Pollen tube growth retardation was observed in the double mutant of expansin genes (*atexpa4 atexpb5*) in Arabidopsis [79]. The mutation of *rsw1* that encodes cellulose synthase reduced cellulose production and exhibited an abnormal phenotype in Arabidopsis [80]. Plant cell walls contain cellulose as a major component. Cellulose is synthesized by cellulose synthase complex in the plasma membrane [81,82]. Cellulose content was reduced in cellulose-deficient mutants in Arabidopsis [83]. In contrast, overexpression of *CesA6*-like genes in Arabidopsis enhances cellulose contents and wall thickness [84]. Our results concluded that depletion of cell wall proteins component in *OsVTC1-1* RNAi lines may interfere with cell wall synthesis in rice.

5. Conclusions

The characteristics of wild type (WT) and *OsVTC1-1* RNAi lines were studied. The expression of genes in AsA biosynthesis pathway, AsA content, leaf anatomical parameters and mannose and galactose content as a percent of total sugars were decreased in the *OsVTC1-1* RNAi line. Notably, the expression of cell wall-associated proteins was decreased

in the *OsVTC1-1* RNAi line. These results suggest that *OsVTC1-1* plays an essential role in AsA production and affects cell wall sugar composition. The results from this study may be useful in understanding the role of the *OsVTC1-1* gene that is involved in cell walls and other mechanisms and processes in plants.

Supplementary Materials: The following are available online at https://www.mdpi.com/article/10.3390/agronomy12061272/s1, Figure S1: Cell wall sugar composition measurement in wild type (WT) and *OsVTC1-1* RNAi lines from 3-week-old rice. (a) xylose; (b) arabinose; (c) galactose; (d) galacturonic acid; (e) fucose; (f) mannose; (g) glucuronic acid. Bars represent the means and standard errors of three replicates; Figure S2: Heat map representation of the expression patterns of 100 common genes from wild type (WT) and *OsVTC1-1* RNAi lines among three replicates. The color scale on the right represents the fragments per kilobase of transcript per million fragments (FPKM) value. Red and green shows high and low expressions, respectively; Figure S3: Principal Component Analysis (PCA) plot of FPKM value of 100 genes from wild type (WT) and *OsVTC1-1* RNAi lines; Table S1: Summary of RNA-seq data and reads mapping; Table S2: The top 20 upregulated differentially expressed genes in RI1-2 and RI1-3 as ranked by log2FC value; Table S3: FPKM expression values of 100 common genes from wild type (WT) and *OsVTC1-1* RNAi lines with three replicates.

Author Contributions: K.L. (Kanyanat Lamanchai) carried out the experiment and wrote the manuscript; D.L.S. assisted K.L. (Kanyanat Lamanchai) to perform the cell wall sugar composition experiment and analyze the GC/MS data; P.S. helped carry out the anatomical study; N.S. designed the AsA measurement in RNAi lines experiment, suggested the cell wall sugar experiment and revised the manuscript; S.R., K.L. (Kantinan Leetanasaksakul) and S.K. performed proteome and data analysis. C.J. conceived the project, designed the experiments, supervised the research and revised manuscript. All authors have read and agreed to the published version of the manuscript.

Funding: This research and innovation activity is funded by National Research Council of Thailand (NRCT) as of fiscal year 2021 and Kasetsart University Research and Development Institute (KURDI) project FF(KU)5.64. Kanyanat Lamanchai was financially supported by Development and Promotion of Science and Technology Talents Project (DPST).

Institutional Review Board Statement: Not applicable.

Informed Consent Statement: Not applicable.

Data Availability Statement: Not applicable.

Acknowledgments: We gratefully acknowledge Zhijin Zhang from Biotechnology Research Institute, Chinese Academy of Agricultural Sciences, Beijing, China for providing *OsVTC1* RNAi rice seeds in this experiment.

Conflicts of Interest: The authors declare no conflict of interest.

References

1. Zhang, Y. Biological Role of Ascorbate in Plants. In *Ascorbic Acid in Plants*; Springer Briefs in Plant Science; Springer: New York, NY, USA, 2013; pp. 7–33.
2. Smirnoff, N. The Function and Metabolism of Ascorbic Acid in Plants. *Ann. Bot.* **1996**, *78*, 661–669. [CrossRef]
3. Davey, M.W.; Montagu, M.V.; Inz, D.; Sanmartin, M.; Kanellis, A.; Smirnoff, N.; Benzie, I.J.J.; Strain, J.J.; Favell, D.; Fletcher, J. Plant L-ascorbic acid: Chemistry, function, metabolism, bioavailability and effects of processing. *J. Sci. Food Agric.* **2000**, *80*, 825–860. [CrossRef]
4. Liso, R.; Calabrese, G.; Bitonti, M.B.; Arrigoni, O. Relationship between ascorbic acid and cell division. *Exp. Cell Res.* **1984**, *150*, 314–320. [CrossRef]
5. Smirnoff, N.; Wheeler, G.L. Ascorbic Acid in Plants: Biosynthesis and Function. *Crit. Rev. Biochem. Mol. Biol.* **2000**, *35*, 291–314. [CrossRef]
6. Höller, S.; Hajirezaei, M.-R.; von Wirén, N.; Frei, M. Ascorbate metabolism in rice genotypes differing in zinc efficiency. *Planta* **2014**, *239*, 367–379. [CrossRef]
7. Conklin, P.; Norris, S.; Wheeler, G.; Williams, E.; Smirnoff, N.; Last, R. Genetic evidence for the role of GDP-mannose in plant ascorbic acid (vitamin c) biosynthesis. *Proc. Natl. Acad. Sci. USA* **1999**, *96*, 4198–4203. [CrossRef]
8. Qin, H.; Deng, Z.; Zhang, C.; Wang, Y.; Wang, J.; Liu, H.; Zhang, Z.; Huang, R.; Zhang, Z. Rice GDP-mannose pyrophosphorylase OsVTC1-1 and OsVTC1-3 play different roles in ascorbic acid synthesis. *Plant Mol. Biol.* **2016**, *90*, 317–327. [CrossRef]

9. Pavet, V.; Olmos, E.; Kiddle, G.; Mowla, S.; Kumar, S.; Antoniw, J.; Alvarez, M.; Foyer, C. Ascorbic acid deficiency activates cell death and disease resistance responses in Arabidopsis. *Plant Physiol.* **2005**, *139*, 1291–1303. [CrossRef]
10. Veljovic-Jovanovic, S.D.; Pignocchi, C.; Noctor, G.; Foyer, C.H. Low ascorbic acid in the vtc-1 mutant of Arabidopsis is associated with decreased growth and intracellular redistribution of the antioxidant system. *Plant Physiol.* **2001**, *127*, 426–435. [CrossRef]
11. Qin, H.; Wang, Y.; Wang, J.; Liu, H.; Zhao, H.; Deng, Z.; Zhang, Z.; Huang, R.; Zhang, Z. Knocking down the expression of GMPase gene OsVTC1-1 decreases salt tolerance of rice at seedling and reproductive stages. *PLoS ONE* **2016**, *11*, e0168650. [CrossRef]
12. Qi, T.; Liu, Z.; Fan, M.; Chen, Y.; Tian, H.; Wu, D.; Gao, H.; Ren, C.; Song, S.; Xie, D. GDP-D-mannose epimerase regulates male gametophyte development, plant growth and leaf senescence in Arabidopsis. *Sci. Rep.* **2017**, *7*, 10309. [CrossRef]
13. Ma, L.; Wang, Y.; Liu, W.; Liu, Z. Overexpression of an alfalfa GDP-mannose 3,5-epimerase gene enhances acid, drought and salt tolerance in transgenic Arabidopsis by increasing ascorbate accumulation. *Biotechnol. Lett.* **2014**, *36*, 2331–2341. [CrossRef]
14. Fenech, M.; Amorim-Silva, V.; Esteban del Valle, A.; Arnaud, D.; Ruiz-Lopez, N.; Castillo, A.G.; Smirnoff, N.; Botella, M.A. The role of GDP-l-galactose phosphorylase in the control of ascorbate biosynthesis. *Plant Physiol.* **2021**, *185*, 1574–1594. [CrossRef] [PubMed]
15. Zhang, G.Y.; Liu, R.R.; Zhang, C.Q.; Tang, K.X.; Sun, M.F.; Yan, G.H.; Liu, Q.Q. Manipulation of the rice L-galactose pathway: Evaluation of the effects of transgene overexpression on ascorbate accumulation and abiotic stress tolerance. *PLoS ONE* **2015**, *10*, e0125870. [CrossRef] [PubMed]
16. Torabinejad, J.; Donahue, J.; Gunesekera, B.; Allen-Daniels, M.; Gillaspy, G. VTC4 is a bifunctional enzyme that affects myoinositol and ascorbate bosynthesis in plants. *Plant Physiol.* **2009**, *150*, 951–961. [CrossRef] [PubMed]
17. Fanucchi, M.V. Chapter 11—Development of antioxidant and xenobiotic metabolizing enzyme systems. In *The Lung*, 2nd ed.; Harding, R., Pinkerton, K.E., Eds.; Academic Press: Boston, MA, USA, 2014; pp. 223–231.
18. Pehlivan, F. Vitamin C: An antioxidant agent. In *Vitamin C*; IntechOpen: London, UK, 2017.
19. Rajput, V.D.; Harish; Singh, R.K.; Verma, K.K.; Sharma, L.; Quiroz-Figueroa, F.R.; Meena, M.; Gour, V.S.; Minkina, T.; Sushkova, S.; et al. Recent developments in enzymatic antioxidant defence mechanism in plants with special reference to abiotic Stress. *Biology* **2021**, *10*, 267. [CrossRef]
20. Held, M.A.; Jiang, N.; Basu, D.; Showalter, A.M.; Faik, A. Plant cell wall polysaccharides: Structure and biosynthesis. In *Polysaccharides: Bioactivity and Biotechnology*; Ramawat, K.G., Mérillon, J.M., Eds.; Springer International Publishing: Cham, Switzerland, 2015; pp. 3–54.
21. Voiniciuc, C.; Pauly, M.; Usadel, B. Monitoring polysaccharide dynamics in the plant cell wall. *Plant Physiol.* **2018**, *176*, 2590–2600. [CrossRef]
22. Ochoa-Villarreal, M.; Aispuro, E.; Vargas-Arispuro, I.; Martínez-Téllez, M. Plant cell wall polymers: Function, structure and biological activity of their derivatives. *Polymerization* **2012**, *4*, 63–86.
23. Kumar, M.; Atanassov, I.; Turner, S. Functional analysis of cellulose synthase (CESA) protein class specificity. *Plant Physiol.* **2017**, *173*, 970–983. [CrossRef]
24. Zhang, W.; Qin, W.; Li, H.; Wu, A.M. Biosynthesis and transport of nucleotide sugars for plant hemicellulose. *Front. Plant Sci.* **2021**, *12*, 723128. [CrossRef]
25. Scheller, H.V.; Ulvskov, P. Hemicelluloses. *Annu. Rev. Plant Biol.* **2010**, *61*, 263–289. [CrossRef] [PubMed]
26. Harholt, J.; Suttangkakul, A.; Vibe Scheller, H. Biosynthesis of pectin. *Plant Physiol.* **2010**, *153*, 384395. [CrossRef] [PubMed]
27. Yapo, B.M. Pectin rhamnogalacturonan II: On the "small stem with four branches" in the primary cell walls of plants. *Int. J. Carbohydr. Chem.* **2011**, *2011*, 964521. [CrossRef]
28. Yoshida, S.; Forno, D.A.; Cock, J.H.; Gomez, K.A. *Laboratory Manual for Physiological Studies of Rice*, 3rd ed.; International Rice Research Institutes: Manila, Philippines, 1976; pp. 61–66.
29. Gregorio, G.; Senadhira, D.; Mendoza, R. *Screening Rice for Salinity Tolerance*; IRRI Discussion Paper Series; International Rice Research Institute: Los Banos, Philippines, 1997; Volume 22.
30. Livak, K.J.; Schmittgen, T.D. Analysis of relative gene expression data using real-time quantitative PCR and the 2(-Delta Delta C(T)) Method. *Methods* **2001**, *25*, 402–408. [CrossRef]
31. Höller, S.; Ueda, Y.; Wu, L.; Wang, Y.; Hajirezaei, M.R.; Ghaffari, M.R.; von Wirén, N.; Frei, M. Ascorbate biosynthesis and its involvement in stress tolerance and plant development in rice (*Oryza sativa* L.). *Plant Mol. Biol.* **2015**, *88*, 545–560. [CrossRef]
32. Islam, T.; Manna, M.; Kaul, T.; Pandey, S.; Reddy, C.S.; Reddy, M.K. Genome-wide dissection of Arabidopsis and rice for the identification and expression analysis of glutathione peroxidases reveals their stress-specific and overlapping response patterns. *Plant Mol. Biol. Report.* **2015**, *33*, 1413–1427. [CrossRef]
33. Chaipanya, C.; Telebanco-Yanoria, M.J.; Quime, B.; Longya, A.; Korinsak, S.; Korinsak, S.; Toojinda, T.; Vanavichit, A.; Jantasuriyarat, C.; Zhou, B. Dissection of broad-spectrum resistance of the Thai rice variety Jao Hom Nin conferred by two resistance genes against rice blast. *Rice* **2017**, *10*, 18. [CrossRef]
34. Gillespie, K.; Ainsworth, E. Measurement of reduced, oxidized and total ascorbate content in plants. *Nat. Protoc.* **2007**, *2*, 871–874. [CrossRef]
35. Ruzin, S.E. *Plant Microtechnique and Microscopy*; Oxford University Press: New York, NY, USA, 1999.

36. Conklin, P.L.; Gatzek, S.; Wheeler, G.L.; Dowdle, J.; Raymond, M.J.; Rolinski, S.; Isupov, M.; Littlechild, J.A.; Smirnoff, N. *Arabidopsis thaliana* VTC4 encodes L-galactose-1-P phosphatase, a plant ascorbic acid biosynthetic enzyme. *J. Biol. Chem.* **2006**, *281*, 15662–15670. [CrossRef]
37. Merchant, N.; Lyons, E.; Goff, S.; Vaughn, M.; Ware, D.; Micklos, D.; Antin, P. The iPlant collaborative: Cyberinfrastructure for enabling data to discovery for the life sciences. *PLoS Biol.* **2016**, *14*, e1002342. [CrossRef]
38. Goff, S.; Vaughn, M.; McKay, S.; Lyons, E.; Stapleton, A.; Gessler, D.; Matasci, N.; Wang, L.; Hanlon, M.; Lenards, A.; et al. The iPlant collaborative: Cyberinfrastructure for plant biology. *Front. Plant Sci.* **2011**, *2*, 34. [CrossRef] [PubMed]
39. Lowry, O.; Rosebrough, N.; Farr, A.L.; Randall, R. Protein measurement with the folin phenol reagent. *J. Biol. Chem.* **1951**, *193*, 265–275. [CrossRef]
40. Tyanova, S.; Temu, T.; Cox, J. The MaxQuant computational platform for mass spectrometry-based shotgun proteomics. *Nat. Protoc.* **2016**, *11*, 2301–2319. [CrossRef] [PubMed]
41. Saeed, A.I.; Sharov, V.; White, J.; Li, J.; Liang, W.; Bhagabati, N.; Braisted, J.; Klapa, M.; Currier, T.; Thiagarajan, M.; et al. TM4: A free, open-source system for microarray data management and analysis. *BioTechniques* **2003**, *34*, 374–378. [CrossRef]
42. Kassambara, A.; Mundt, F. Extract and Visualize the Results of Multivariate Data Analyses [R Package Factoextra Version 1.0.7]. 2020. Available online: https://CRAN.R-project.org/package=factoextra (accessed on 20 May 2022).
43. Conklin, P.; Saracco, S.; Norris, S.; Last, R. Identification of ascorbic acid-deficient *Arabidopsis thaliana* Mutants. *Genetics* **2000**, *154*, 847–856. [CrossRef]
44. Keller, R.; Renz, F.S.; Kossmann, J. Antisense inhibition of the GDP-mannose pyrophosphorylase reduces the ascorbate content in transgenic plants leading to developmental changes during senescence. *Plant J.* **1999**, *19*, 131–141. [CrossRef]
45. Wang, H.-S.; Yu, C.; Zhu, Z.-J.; Yu, X.-C. Overexpression in tobacco of a tomato *GMPase* gene improves tolerance to both low and high temperature stress by enhancing antioxidation capacity. *Plant Cell Rep.* **2011**, *30*, 1029–1040. [CrossRef]
46. Badejo, A.A.; Tanaka, N.; Esaka, M. Analysis of GDP-d-mannose pyrophosphorylase gene promoter from acerola (*Malpighia glabra*) and increase in ascorbate content of transgenic tobacco expressing the acerola gene. *Plant Cell Physiol.* **2008**, *49*, 126–132. [CrossRef]
47. Zhou, Y.; Tao, Q.C.; Wang, Z.N.; Fan, R.; Li, Y.; Sun, X.F.; Tang, K.X. Engineering ascorbic acid biosynthetic pathway in Arabidopsis leaves by single and double gene transformation. *Biol. Plant.* **2012**, *56*, 451–457. [CrossRef]
48. Cronje, C.; George, G.; Fernie, A.; Bekker, J.; Kossmann, J.; Bauer, R. Manipulation of L-ascorbic acid biosynthesis pathways in *Solanum lycopersicum*: Elevated GDP-mannose pyrophosphorylase activity enhances L-ascorbate levels in red fruit. *Planta* **2012**, *235*, 553–564. [CrossRef]
49. Gilbert, L.; Alhagdow, M.; Nunes-Nesi, A.; Quéméner, B.; Guillon, F.; Bouchet, B.; Faurobert, M.; Gouble, B.; Page, D.; Garcia, V.; et al. GDP-D-mannose 3,5-epimerase (GME) plays a key role at the intersection of ascorbate and non-cellulosic cell-wall biosynthesis in tomato. *Plant J.* **2009**, *60*, 499–508. [CrossRef] [PubMed]
50. Lim, B.; Smirnoff, N.; Cobbett, C.; Golz, J. Ascorbate-deficient vtc2 mutants in Arabidopsis do not exhibit decreased growth. *Front. Plant Sci.* **2016**, *7*, 1025. [CrossRef] [PubMed]
51. Li, X.; Ye, J.; Munir, S.; Yang, T.; Chen, W.; Liu, G.; Zheng, W.; Zhang, Y. Biosynthetic gene pyramiding leads to ascorbate accumulation with enhanced oxidative stress tolerance in tomato. *Int. J. Mol. Sci.* **2019**, *20*, 1558. [CrossRef] [PubMed]
52. Gatzek, S.; Wheeler, G.; Smirnoff, N. Antisense suppression of L-galactose dehydrogenase in *Arabidopsis thaliana* provides evidence for its role in ascorbate synthesis and reveals light modulated L-galactose synthesis. *Plant J.* **2002**, *30*, 541–553. [CrossRef] [PubMed]
53. Foyer, C.H.; Noctor, G. Ascorbate and glutathione: The heart of the redox hub. *Plant Physiol.* **2011**, *155*, 2–18. [CrossRef]
54. Potters, G.; De Gara, L.; Asard, H.; Horemans, N. Ascorbate and glutathione: Guardians of the cell cycle, partners in crime? *Plant Physiol. Biochem.* **2002**, *40*, 537–548. [CrossRef]
55. Mellidou, I.; Koukounaras, A.; Kostas, S.; Patelou, E.; Kanellis, A.K. Regulation of vitamin C accumulation for improved tomato fruit quality and alleviation of abiotic stress. *Genes* **2021**, *12*, 694. [CrossRef]
56. Zhang, H.; Li, A.; Zhang, Z.; Huang, Z.; Lu, P.; Zhang, D.; Liu, X.; Zhang, Z.-F.; Huang, R. Ethylene response factor TERF1, regulated by ethylene-insensitive3-like factors, functions in reactive oxygen species (ROS) scavenging in tobacco (*Nicotiana tabacum* L.). *Sci. Rep.* **2016**, *6*, 29948. [CrossRef]
57. Ortiz-Espín, A.M.; Sánchez Guerrero, A.; Sevilla, F.; Jiménez, A. The role of ascorbate in plant growth and development. In *Ascorbic Acid in Plant Growth, Development and Stress Tolerance*; Springer: Cham, Switzerland, 2017; pp. 25–45.
58. Shih, M.C.; Chang, C.M.; Kang, S.M.; Tsai, M.L. Effect of different parts (leaf, stem and stalk) and seasons (summer and winter) on the chemical compositions and antioxidant activity of *Moringa oleifera*. *Int. J. Mol. Sci.* **2011**, *12*, 6077–6088. [CrossRef]
59. Kka, N.; Rookes, J.; Cahill, D. Quantitation of ascorbic acid in *Arabidopsis thaliana* reveals distinct differences between organs and growth phases. *Plant Growth Regul.* **2017**, *81*, 283–292. [CrossRef]
60. Arrigoni, O. Ascorbate system in plant development. *J. Bioenerg. Biomembr.* **1994**, *26*, 407–419. [CrossRef] [PubMed]
61. Tommasi, F.; Paciolla, C.; de Pinto, M.; De Gara, L. A comparative study of glutathione and ascorbate metabolism during germination of *Pinus pinea* L. seeds. *J. Exp. Bot.* **2001**, *52*, 1647–1654. [CrossRef] [PubMed]
62. Zechmann, B.; Stumpe, M.; Mauch, F. Immunocytochemical determination of the subcellular distribution of ascorbate in plants. *Planta* **2011**, *233*, 1–12. [CrossRef]

63. Antonova, G. The role of ascorbate in growth and development of cells during the formation of annual rings in coniferous trees. In *Oxidative Stress in Plants: Causes, Consequences and Tolerance*; IK International Publishing House: New Delhi, India, 2011.
64. Cárcamo, H.J.; Bustos, R.M.; Fernández, F.E.; Bastías, E. Mitigating effect of salicylic acid in the anatomy of the leaf of *Zea mays* L. lluteño ecotype from the Lluta valley (Arica-Chile) under NaCl stress. *Idesia* **2012**, *30*, 55–63. [CrossRef]
65. Schädel, C.; Blöchl, A.; Richter, A.; Hoch, G. Quantification and monosaccharide composition of hemicelluloses from different plant functional types. *Plant Physiol. Biochem.* **2010**, *48*, 1–8. [CrossRef]
66. Lukowitz, W.; Nickle, T.C.; Meinke, D.W.; Last, R.L.; Conklin, P.L.; Somerville, C.R. Arabidopsis cyt1 mutants are deficient in a mannose-1-phosphate guanylyltransferase and point to a requirement of N-linked glycosylation for cellulose biosynthesis. *Proc. Natl. Acad. Sci. USA* **2001**, *98*, 2262–2267. [CrossRef] [PubMed]
67. Gibeaut, D.M.; Carpita, N.C. Biosynthesis of plant cell wall polysaccharides. *Faseb J.* **1994**, *8*, 904–915. [CrossRef]
68. Ciereszko, I. Regulatory roles of sugars in plant growth and development. *Acta Soc. Bot. Pol.* **2018**, *87*. [CrossRef]
69. Pastori, G.M.; Kiddle, G.; Antoniw, J.; Bernard, S.; Veljovic-Jovanovic, S.; Verrier, P.J.; Noctor, G.; Foyer, C.H. Leaf vitamin C contents modulate plant defense transcripts and regulate genes that control development through hormone signaling. *Plant Cell* **2003**, *15*, 939–951. [CrossRef]
70. Newsholme, P.; Stenson, L.; Sulvucci, M.; Sumayao, R.; Krause, M. 1.02—Amino Acid Metabolism. In *Comprehensive Biotechnology (Second Edition)*; Moo-Young, M., Ed.; Academic Press: Burlington, NJ, USA, 2011; pp. 3–14.
71. Rosenberg, E.; Filer, D.; Zafriti, D.; Kindler, S.H. Aspartokinase activity and the developmental cycle of *Myxococcus xanthus*. *J. Bacteriol.* **1973**, *115*, 29–34. [CrossRef]
72. Mo, C.; Wan, S.; Xia, Y.; Ren, N.; Zhou, Y.; Jiang, X. Expression patterns and identified protein-protein interactions suggest that cassava CBL-CIPK signal networks function in responses to abiotic stresses. *Front. Plant Sci.* **2018**, *9*. [CrossRef]
73. Wang, P.; Hsu, C.-C.; Du, Y.; Zhu, P.; Zhao, C.; Fu, X.; Zhang, C.; Paez, J.S.; Macho, A.P.; Tao, W.A.; et al. Mapping proteome-wide targets of protein kinases in plant stress responses. *Proc. Natl. Acad. Sci. USA* **2020**, *117*, 3270–3280. [CrossRef] [PubMed]
74. Wilson, B.J.; Gray, A.C.; Matthews, B.F. Bifunctional protein in carrot contains both aspartokinase and homoserine dehydrogenase activities. *Plant Physiol.* **1991**, *97*, 1323–1328. [CrossRef] [PubMed]
75. Tam, J.P.; Wang, S.; Wong, K.H.; Tan, W.L. Antimicrobial peptides from plants. *Pharmaceuticals* **2015**, *8*, 711–757. [CrossRef] [PubMed]
76. Pruzinská, A.; Tanner, G.; Anders, I.; Roca, M.; Hörtensteiner, S. Chlorophyll breakdown: Pheophorbide a oxygenase is a rieske-type iron-sulfur protein, encoded by the accelerated cell death 1 gene. *Proc. Natl. Acad. Sci. USA* **2003**, *100*, 15259–15264. [CrossRef] [PubMed]
77. Webber, A.N.; Packman, L.C.; Gray, J.C. A 10 kDa polypeptide associated with the oxygen-evolving complex of photosystem II has a putative C-terminal non-cleavable thylakoid transfer domain. *FEBS Lett.* **1989**, *242*, 435–438. [CrossRef]
78. McQueen-Mason, S.; Cosgrove, D.J. Disruption of hydrogen bonding between plant cell wall polymers by proteins that induce wall extension. *Proc. Natl. Acad. Sci. USA* **1994**, *91*, 6574–6578. [CrossRef]
79. Liu, W.; Xu, L.; Lin, H.; Cao, J. Two expansin genes, AtEXPA4 and AtEXPB5, are redundantly required for pollen tube growth and AtEXPA4 is involved in primary root elongation in *Arabidopsis thaliana*. *Genes* **2021**, *12*, 249. [CrossRef]
80. Arioli, T.; Peng, L.; Betzner, A.S.; Burn, J.; Wittke, W.; Herth, W.; Camilleri, C.; Höfte, H.; Plazinski, J.; Birch, R.; et al. Molecular analysis of cellulose biosynthesis in Arabidopsis. *Science* **1998**, *279*, 717–720. [CrossRef]
81. Paredez, A.R.; Somerville, C.R.; Ehrhardt, D.W. Visualization of cellulose synthase demonstrates functional association with microtubules. *Science* **2006**, *312*, 1491–1495. [CrossRef]
82. Taylor, N.G. Cellulose biosynthesis and deposition in higher plants. *New Phytol.* **2008**, *178*, 239–252. [CrossRef] [PubMed]
83. Kumar, M.; Mishra, L.; Carr, P.; Pilling, M.; Gardner, P.; Mansfield, S.D.; Turner, S. Exploiting cellulose synthase (CESA) class specificity to probe cellulose microfibril biosynthesis. *Plant Physiol.* **2018**, *177*, 151–167. [CrossRef] [PubMed]
84. Hu, H.; Zhang, R.; Feng, S.; Wang, Y.; Wang, Y.; Fan, C.; Ying, L.; Liu, Z.; Schneider, R.; Xia, T.; et al. Three AtCesA6-like members enhance biomass production by distinctively promoting cell growth in Arabidopsis. *Plant Biotechnol. J.* **2017**, *16*, 976–988. [CrossRef] [PubMed]